13. Barikot in Context

Luca M. Olivieri

URL: https://shahi.pubpub.org/pub/hl440b2k

License: Creative Commons Attribution-NonCommercial-NoDerivatives 4.0 International License (CC-BY-NC-ND 4.0)

Exploring the Contributions of the Shahi Kingdoms to Inner and South Asia

Final publication of the Austrian Science Fund (FWF) project (P-31246) "Cultural Formation and Transformation: Shahi Art and Architecture from Afghanistan to the West Tibetan Frontier at the Dawn of the Islamic Era."

Chapter 13. Barikot in Context

Author(s): Luca M. Olivieri

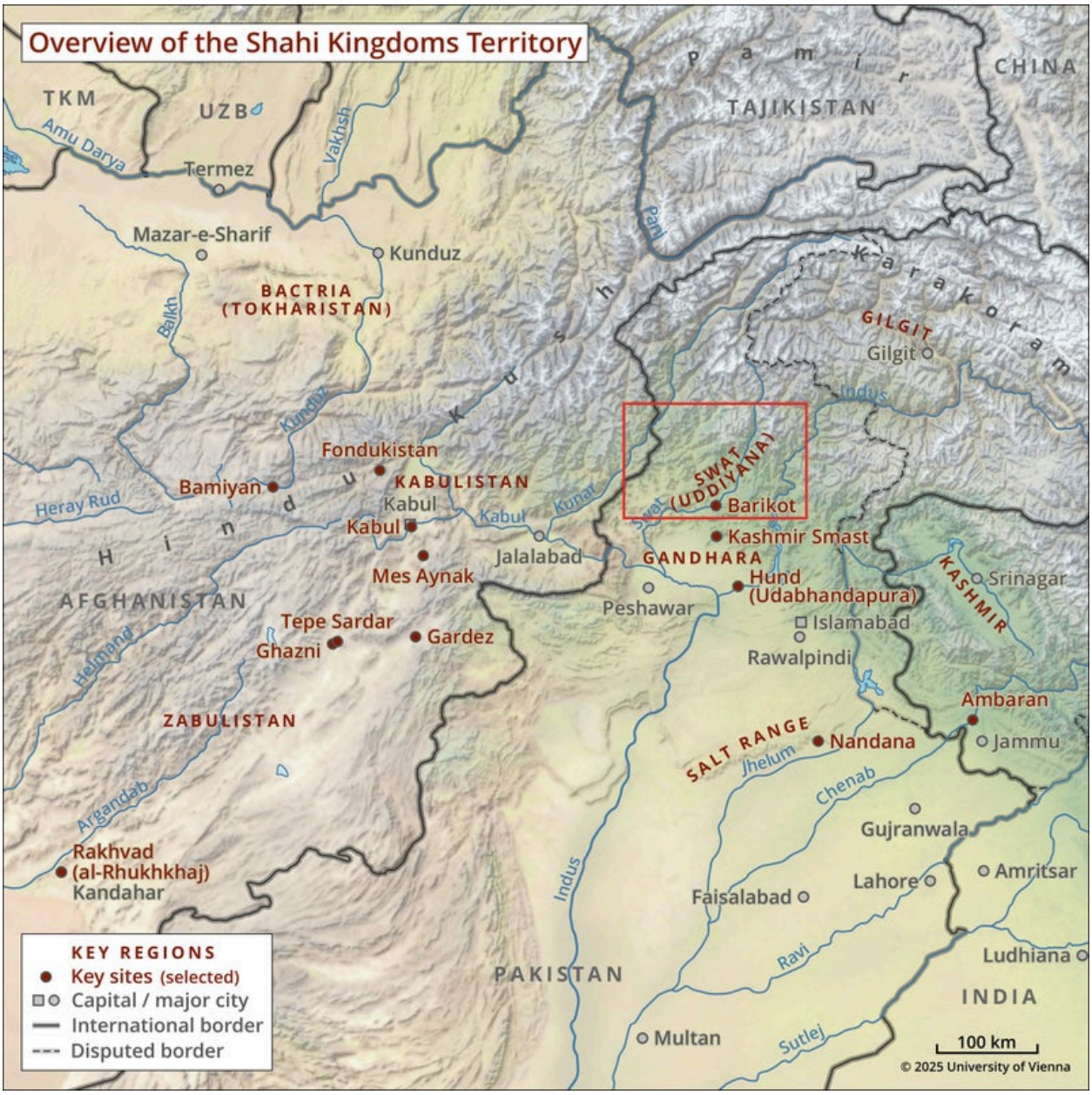

Map 13–19. Key regions of the Shahi territories discussed in chapters 13–19 (University of Vienna, Department of Geography and Regional Research, 2025, with annotations, CC BY-NC-ND 4.0)

> *There is no natural feature of the country [i.e., Swat] which has not been turned to advantage. The immense flats are flooded periodically as of old and produce a rice harvest second to none in India.*
>
> Alexander E. Caddy Esq. on special duty to the Chief Secretary of the Government of Bengal. Dated Camp Chakdara [Swat], May 13th, 1896.[1]

Geography

The Swat Valley is a large mountainous valley of the Hindukush/Karakoram, uniquely oriented east-west, that is, transversely to the mountain ranges (**Fig. 1**). The reason for this anomaly is quickly stated: “A major fault, the Main Mantle Thrust (MMT) strikes east-west across the Swat Valley, separates regions of markedly differing fission-track age regimes, and may be a suture zone separating an extinct island arc terrane on the north from the Indian plate to the south” (Zeitler et al. 1982: 227).

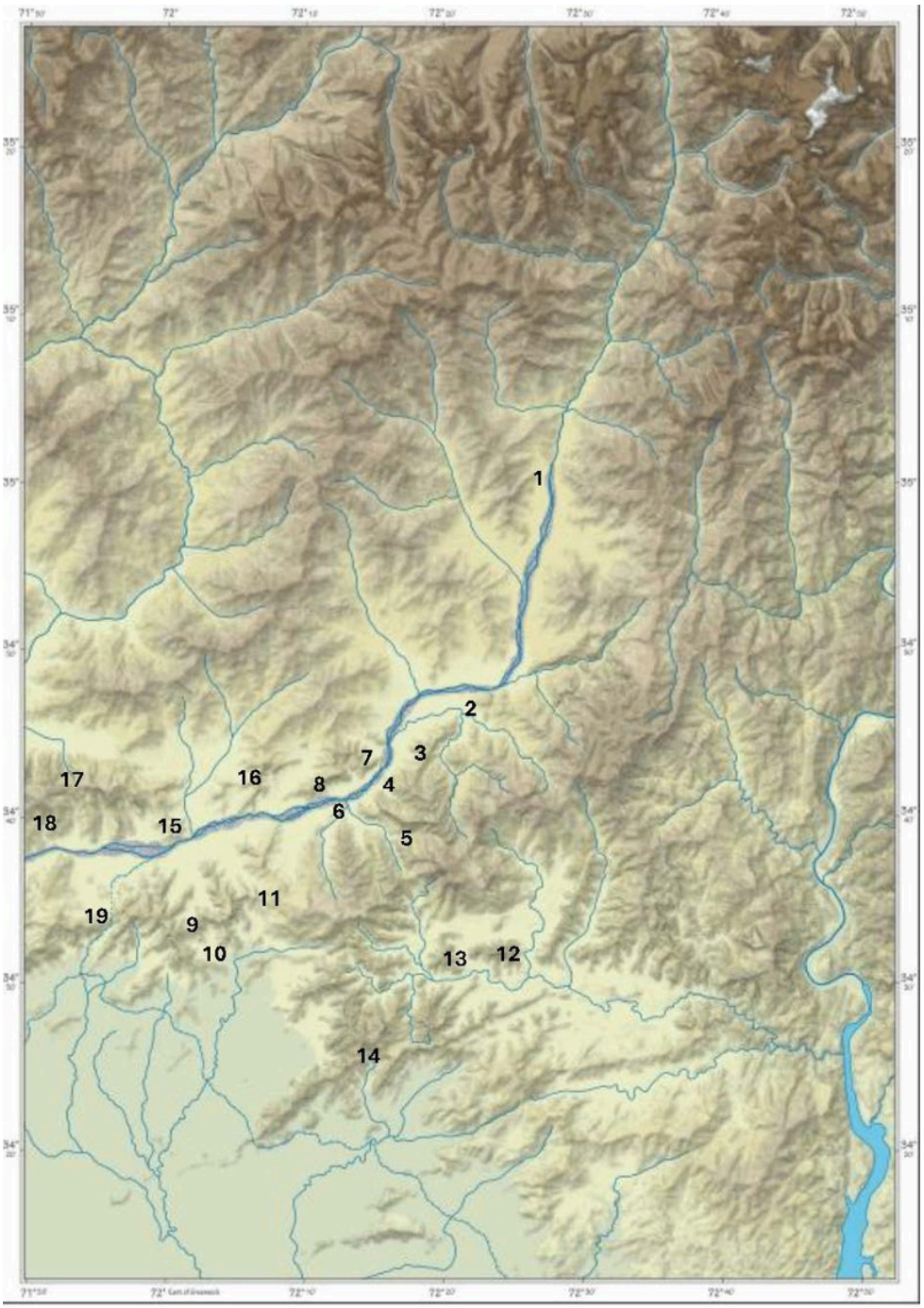

Fig. 1. Map of Swat, Pakistan with the position of some of the major sites described in the following pages: 1, Sure Tangai; 2, Mingora; 3, Udegram; 4, Manyar; 5, Amluk Dara; 6, Barikot; 7, Bar Tangai; 8, Parrai; 9, Zalamkot; 10, Palai; 11, Cherat; 12, Torwarsak; 13, Kingargai; 14, Kashmir Smast; 15, Damkot; 16, Kamal-khan-china; 17, Gumbatuna; 18, Mane Tangai; 19, Malakand (map by K. Kriz and D. Nell, University of Vienna/Courtesy IAMP)

Fig. 2. View of Barikot and the Swat Valley from the southwest (IAMP, CC BY-NC-ND 4.0)

Bordered on all sides by mountains, the Swat Valley is large and secluded, akin to a highland plain comparable to Kashmir rather than a mountain valley, as the celebrated Pashtun poet Kushal Khan Khattak (1613–1689) wrote in the seventeenth century (Khattak, *Swātnāma*, 1.13) (**Fig. 2**).

The valley is, therefore, a closed environment with no natural outlets other than those created by the strain of the waters (the Swat River flows through extremely narrow gorges). These special conditions, similar to those of a closed basin, have allowed the loess deposits, rich in nitrogen, salts, and minerals, to grow *in situ* instead of being washed away. In this way, a kind of time capsule was created that allowed the preservation of geological and human history in a way not possible elsewhere. In addition to this, the combination of long sunshine, incredibly fertile and naturally irrigated soils, and special microclimatic conditions has created the conditions for an agricultural paradise. The main agricultural centers of Swat, characterized by large expanses of lowland, are Kabbal, Damghar, and Matta on the right bank, and Thana, Mingora, and Barikot on the left bank.

The city of Barikot (Bīr-koṭ; ca. 800 meters a.s.l) lies in the Middle Valley of the Swat River, the ancient region of Uddiyana (Uḍiyāna or Oḍiyāna; **Fig. 1**). The site is marked by a hill (*ghwaṇḍai* in Pashto; 942 meters a.s.l.) that stands isolated like a diamond in the fertile water-rich valley of the Swat River (Iori 2023: 103) (**Fig. 2**). Barikot's hinterland comprises three side valleys—Karakar, Kotah, and Kandak—and includes some fertile lands on the opposite left bank.

The role of double-crop agriculture and the valley's immense fertility, thanks to the massive Pleistocene deposits of loess, were celebrated in antiquity (Barikot was "*urbs opulenta*" in the words of Curtius Rufus) and were the reasons for the early phase of urbanization documented in Barikot from the sixth–fifth century BCE. Barikot became an agricultural colony, a center that administered an unsurpassed economic resource for the benefit of the settlements that dotted the great trade route from Afghanistan to India along the Kabul River (for the route, see Inaba, chapter 3). In fact, these Gandharan territories are semi-arid flat lands, which traditionally depended on the monsoon for agricultural production (monoculture/*kharif* cultivation). Those located on the northern hilly plateaus (Bajaur, Swat/Malakand) offered and still offer more stable conditions for double-crop production. For this reason, Pushkalavati (Charsadda), and later Purushapura (Peshawar), which are located in the monoculture ecological zone, could depend for their livelihoods on the double cropping and agricultural production of the hilly areas and, in particular, of Swat. These aspects have been addressed in depth in several recent publications (Olivieri and Iori 2021a; Olivieri 2020a; 2025b).

Fig. 3. View of the Barikot hill from the southeast (after Barger and Wright 1942: pl. 1.2)

The spatial context we are dealing with is that of a steep hill to the north of the present village of Barikot. The profile of the hill presents a heavily eroded lime schist escarpment that becomes vertical to the south (the flank overlooking the plain of the ancient lower town). The northern flank presents a marked gradient profile toward the Swat River, featuring a 45-degree slide of garnet mica schist rocks (**Fig. 3**).

Name(s) and Chronology of the Site

Barikot is a large multiphase archaeological site (ca. 15 hectares) identified with the ancient town of Bazira/Beira (**Fig. 4**). The latter was a town with a large (ca. 12 hectares) lower city, surrounded since early historic times by an urban defense, and an acropolis, located on the hill (ca. 2 hectares). The ancient city was defined as "*poleis*" or "*urbs opulenta*" by the ancient sources of Alexander the Great (see refs. in Stein 1930: 28–29, 40–41; Tucci 1958: 288, 296, 327 n. 28; De Chiara 2020: 79–81; see also Olivieri and Tribulato 2017; Coloru and Olivieri 2019; Olivieri and Iori 2021a).

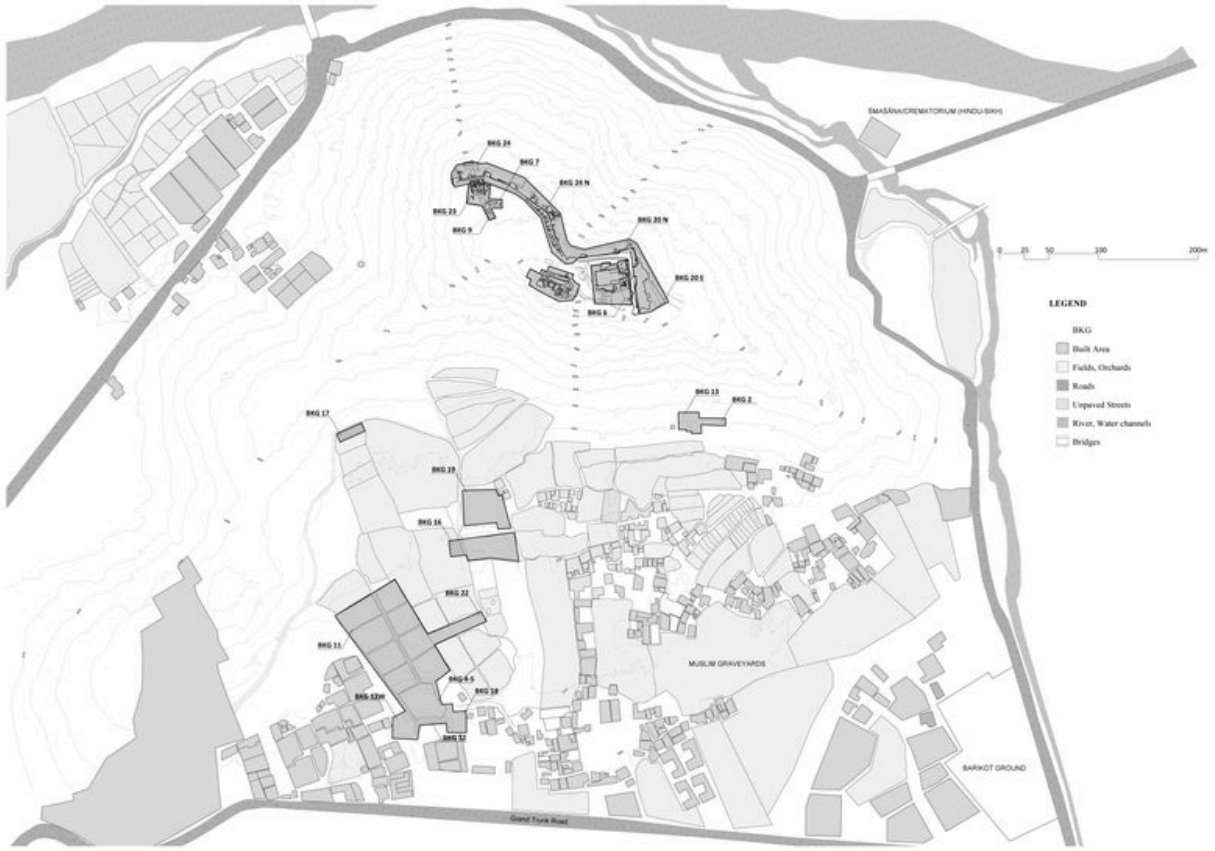

Fig. 4. General map of the Barikot site with excavation areas (EssaNoor Associates/IAMP, CC BY-NC-ND 4.0)

The names Bazira/Beira reported in those sources are the phonetic transcription of a toponym known in the Sanskrit and Prakrit, respectively, as Vajra and Vaïra: "diamond," "thunderbolt." This was how the ancient name of the urban settlement was locally pronounced ("*Beira incolae vocant*," according to Curtius Rufus, VIII 10, 22; Baums 2019: 169–170).

The site is mentioned as Vajirasthana ("the fortified place of Vajra") in a Shahi-era inscription found at Barikot in 1899 and now in the Lahore Museum (LM 119; von Hinüber in Olivieri 2020b; Morgan and Olivieri 2023). It presents an extremely fragmentary text, which preserves in line 2 the name of Shahi king

Jayapala Deva (late 10th century CE), the place name of Vajirasthana, and in line 3 mentions three individuals who patronized the reconstruction of a religious building (locative: "*devakule*") (Sahni 1931–32: 293–301; also Holz and Strauch, chapter 2) (**Fig. 5**).

Fig. 5. The Inscription LM 119 (IAMP; courtesy Lahore Museum, CC BY-NC-ND 4.0)

The fifteenth-century Tibetan *Blue Annals* mentions Vajirastana as a city associated with the name of the legendary seventh-century CE king Indrabhuti. There "[...] in the northern quarter, in Śrī-Vajrasthāna, Oḍḍīyāna [Swat]" Tantric Buddhism was best taught (Roerich 1949: 361; see Olivieri 2022a: 220–221, n. 7).

We can only guess why the hill has been associated with the *vajra* since prehistoric times.[2] It may have been because of its shape, which emerges isolated like a diamond in the middle of the Swat Valley (Iori 2023); because of the primordial splendor associated with its ancient, glittering, sharp profile;[3] and perhaps because of the lightning and St. Elmo's fires that it occasionally attracts to its summit during late summer dry electrical storms.

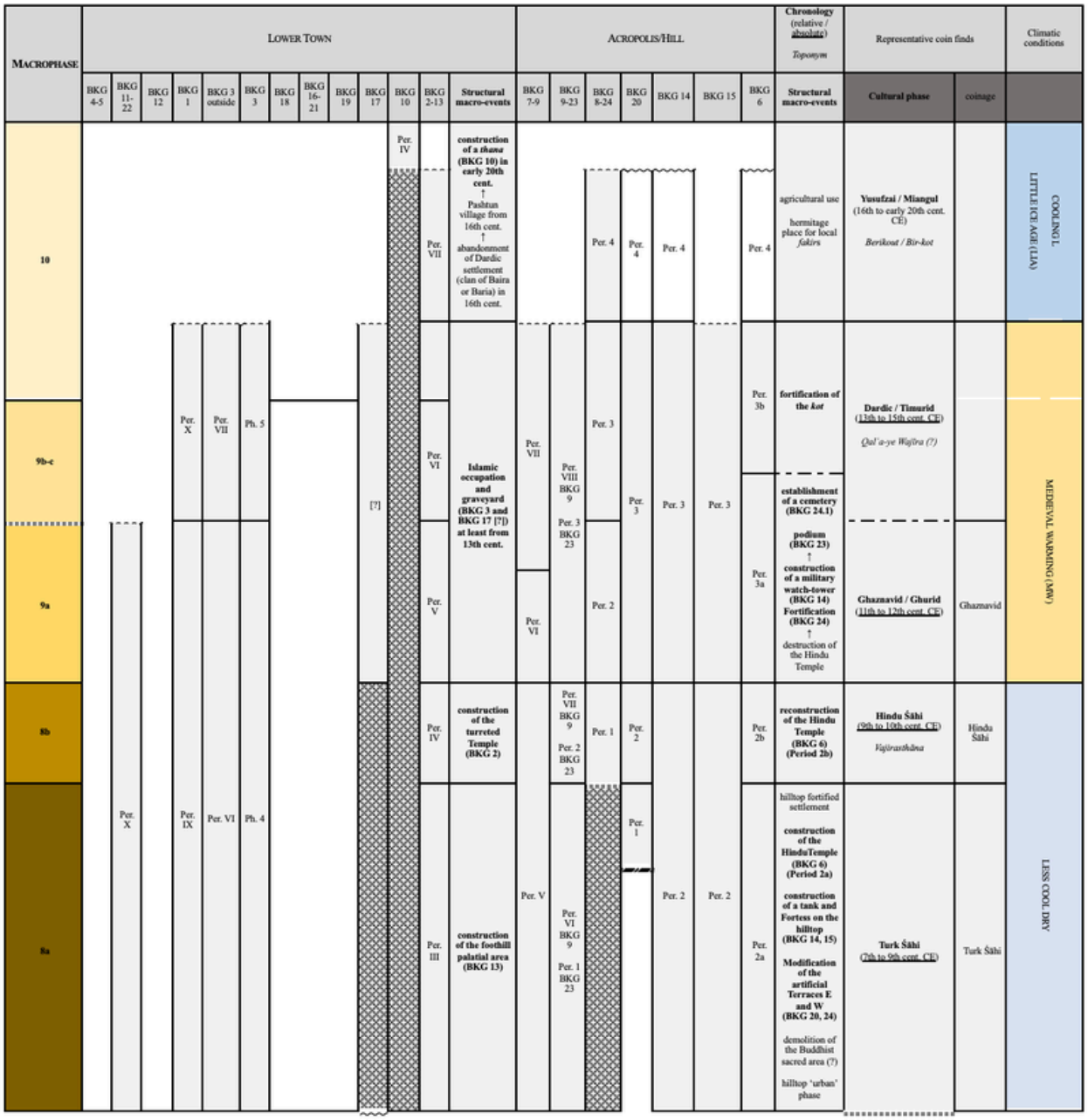
Macrophase
Lower Town
Acropolis/Hill
Chronology (relative / absolute)
Toponym
Representative coin finds
Climatic conditions
BKG 4-5
BKG 11-22
BKG 12
BKG 1
BKG 3 outside
BKG 3
BKG 18
BKG 16-21
BKG 19
BKG 17
BKG 10
BKG 2-13
Structural macro-events
BKG 7-9
BKG 9-23
BKG 8-24
BKG 20
BKG 14
BKG 15
BKG 6
Structural macro-events
Cultural phase
coinage
10
9b-c
9a
8b
8a
Per. IV
Per. VII
Per. X
Per. VII
Ph. 5
[?]
Per. VI
Per. V
Per. IV
Per. III
Per. X
Per. IX
Per. VI
Ph. 4
construction of a thana (BKG 10) in early 20th cent.
↑
Pashtun village from 16th cent.
↑
abandonment of Dardic settlement (clan of Baira or Baria) in 16th cent.
Islamic occupation and graveyard (BKG 3 and BKG 17 [?]) at least from 13th cent.
construction of the turreted Temple (BKG 2)
construction of the foothill palatial area (BKG 13)
Per. VII
Per. VI
Per. V
Per. VII BKG 9
Per. 2 BKG 23
Per. VIII BKG 9
Per. 3 BKG 23
Per. VI BKG 9
Per. 1 BKG 23
Per. 4
Per. 3
Per. 2
Per. 1
Per. 4
Per. 4
Per. 3
Per. 2
Per. 4
Per. 3
Per. 3
Per. 2
Per. 3b
Per. 3a
Per. 2b
Per. 2a
agricultural use
hermitage place for local fakirs
fortification of the kot
establishment of a cemetery (BKG 24.1)
podium (BKG 23)
↑
construction of a military watch-tower (BKG 14)
Fortification (BKG 24)
↑
destruction of the Hindu Temple
reconstruction of the Hindu Temple (BKG 6) (Period 2b)
hilltop fortified settlement
construction of the HinduTemple (BKG 6) (Period 2a)
construction of a tank and Fortess on the hilltop (BKG 14, 15)
Modification of the artificial Terraces E and W (BKG 20, 24)
demolition of the Buddhist sacred area (?)
hilltop 'urban' phase
Yusufzai / Miangul (16th to early 20th cent. CE)
Barikoat / Bir-kot
Dardic / Timurid (13th to 15th cent. CE)
Qal'a-ye Wāǰīra (?)
Ghaznavid / Ghurid (11th to 12th cent. CE)
Hindu Šāhi (9th to 10th cent. CE)
Vāǰīrasthāna
Turk Šāhi (7th to 9th cent. CE)
Ghaznavid
Hindu Šāhi
Turk Šāhi
COOLING L
LITTLE ICE AGE (LIA)
MEDIEVAL WARMING (MW)
LESS COOL DRY

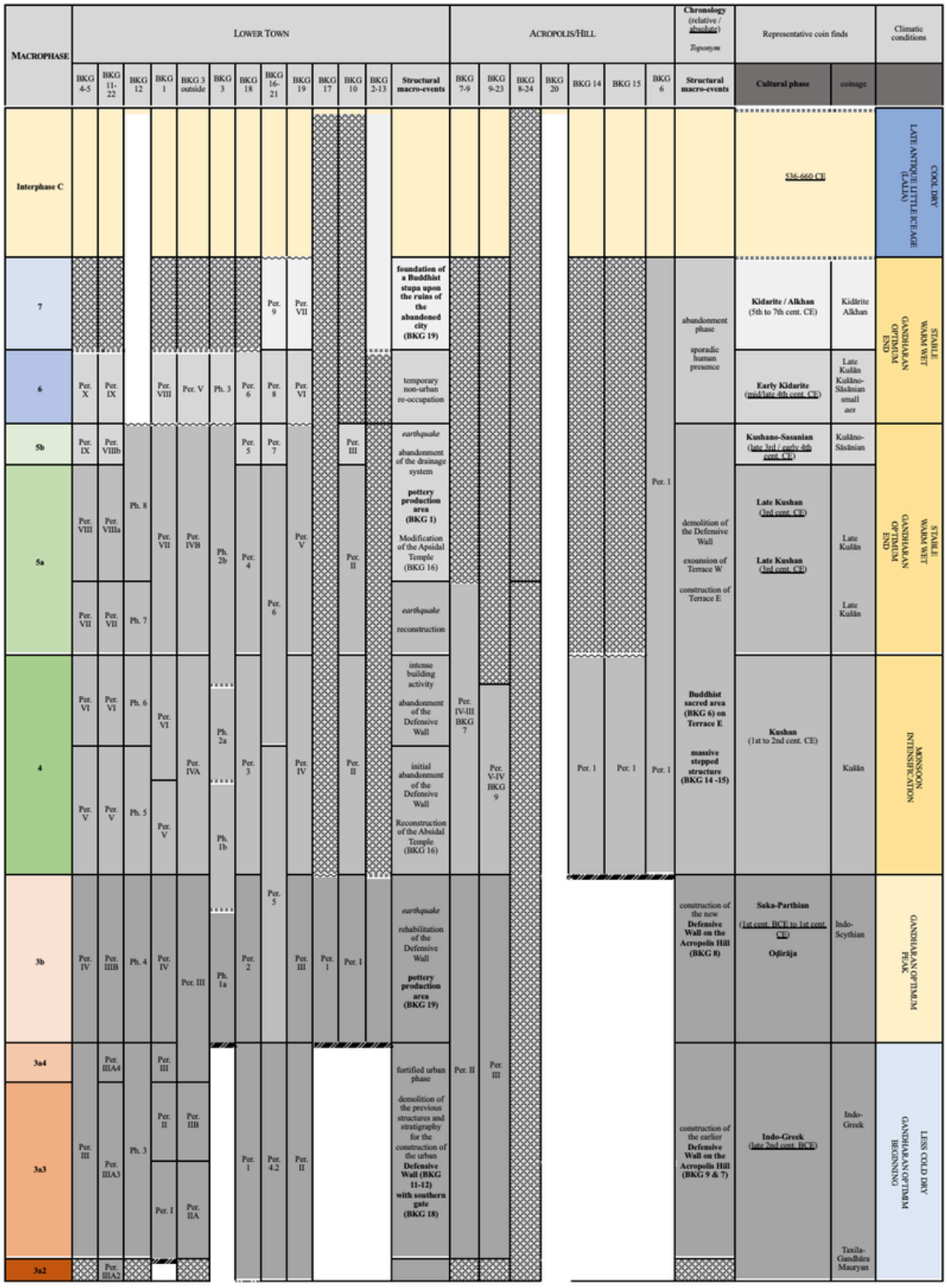
MACROPHASE
LOWER TOWN
ACROPOLIS/HILL
Chronology (relative / absolute)
Toponym
Representative coin finds
Climatic conditions
BKG 4-5
BKG 11-22
BKG 12
BKG 1
BKG 3 outside
BKG 3
BKG 18
BKG 16-21
BKG 19
BKG 17
BKG 10
BKG 2-13
Structural macro-events
BKG 7-9
BKG 9-23
BKG 8-24
BKG 20
BKG 14
BKG 15
BKG 6
Structural macro-events
Cultural phase
coinage
Interphase C
536-660 CE
COOL DRY
LATE ANTIQUE LITTLE ICE AGE (LALIA)
7
foundation of a Buddhist stupa upon the ruins of the abandoned city (BKG 19)
abandonment phase
sporadic human presence
Kidarite / Alkhan (5th to 7th cent. CE)
Kidārite Alkhan
6
temporary non-urban re-occupation
Early Kidarite (mid/late 4th cent. CE)
Late Kuṣān Kuṣāno-Sāsānian small aes
STABLE WARM WET GANDHARAN OPTIMUM END
5b
earthquake
abandonment of the drainage system
pottery production area (BKG 1)
Kushano-Sasanian (late 3rd / early 4th cent. CE)
Kuṣāno-Sāsānian
5a
Modification of the Apsidal Temple (BKG 16)
demolition of the Defensive Wall
exoansion of Terrace W
construction of Terrace E
Late Kushan (2nd cent. CE)
Late Kushan (2nd cent. CE)
Late Kuṣān
Late Kuṣān
earthquake
reconstruction
4
intense building activity
abandonment of the Defensive Wall
initial abandonment of the Defensive Wall
Reconstruction of the Absidal Temple (BKG 16)
Buddhist sacred area (BKG 6) on Terrace E
massive stepped structure (BKG 14 -15)
Kushan (1st to 2nd cent. CE)
Kuṣān
MONSOON INTENSIFICATION
3b
earthquake
rehabilitation of the Defensive Wall
pottery production area (BKG 19)
construction of the new Defensive Wall on the Acropolis Hill (BKG 8)
Saka-Parthian (1st cent. BCE to 1st cent. CE)
Oḍirāja
Indo-Scythian
GANDHARAN OPTIMUM PEAK
3a4
fortified urban phase
3a3
demolition of the previous structures and stratigraphy for the construction of the urban Defensive Wall (BKG 11-12) with southern gate (BKG 18)
construction of the earlier Defensive Wall on the Acropolis Hill (BKG 9 & 7)
Indo-Greek (late 2nd cent. BCE)
Indo-Greek
LESS COLD DRY GANDHARAN OPTIMM BEGINNING
3a2
Taxila-Gandhāra Mauryan

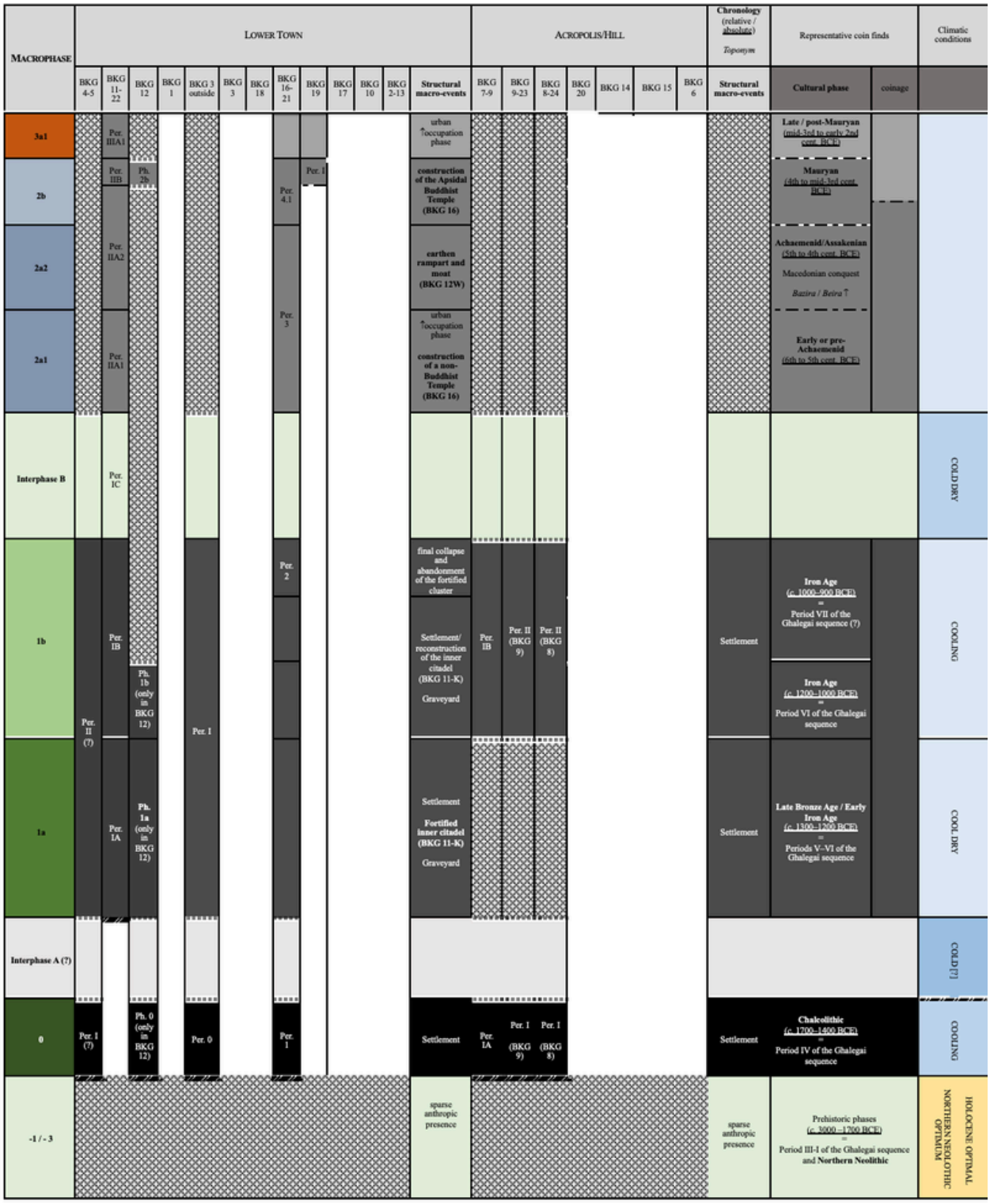
Macrophase
Lower Town
Acropolis/Hill
Chronology (relative / absolute)
Toponym
Representative coin finds
Climatic conditions
BKG 4-5
BKG 11-22
BKG 12
BKG 1
BKG 3 outside
BKG 3
BKG 18
BKG 16-21
BKG 19
BKG 17
BKG 10
BKG 2-13
Structural macro-events
BKG 7-9
BKG 9-23
BKG 8-24
BKG 20
BKG 14
BKG 15
BKG 6
Structural macro-events
Cultural phase
coinage
3a1
2b
2a2
2a1
Interphase B
1b
1a
Interphase A (?)
0
-1 / -3
Per. IIIA1
Per. IIB
Per. IIA2
Per. IIA1
Per. IC
Per. II (?)
Per. IB
Per. 1A
Per. I (?)
Ph. 2b
Ph. 1b (only in BKG 12)
Ph. 1a (only in BKG 12)
Ph. 0 (only in BKG 12)
Per. I
Per. 0
Per. 4.1
Per. 3
Per. 2
Per. 1
Per. I
urban ↑occupation phase
construction of the Apsidal Buddhist Temple (BKG 16)
earthen rampart and moat (BKG 12W)
urban ↑occupation phase
construction of a non-Buddhist Temple (BKG 16)
final collapse and abandonment of the fortified cluster
Settlement/ reconstruction of the inner citadel (BKG 11-K)
Graveyard
Settlement
Fortified inner citadel (BKG 11-K)
Graveyard
Settlement
sparse anthropic presence
Per. IB
Per. II (BKG 9)
Per. II (BKG 8)
Per. IA
Per. I (BKG 9)
Per. I (BKG 8)
sparse anthropic presence
Late / post-Mauryan (mid-3rd to early 2nd cent. BCE)
Mauryan (4th to mid-3rd cent. BCE)
Achaemenid/Assakenian (5th to 4th cent. BCE)
Macedonian conquest
Bazira / Beira ↑
Early or pre-Achaemenid (6th to 5th cent. BCE)
Iron Age (c. 1000–900 BCE) = Period VII of the Ghalegai sequence (?)
Iron Age (c. 1200–1000 BCE) = Period VI of the Ghalegai sequence
Late Bronze Age / Early Iron Age (c. 1300–1200 BCE) = Periods V–VI of the Ghalegai sequence
Chalcolithic (c. 1700–1400 BCE) = Period IV of the Ghalegai sequence
Prehistoric phases (c. 3000–1700 BCE) = Period III-I of the Ghalegai sequence and Northern Neolithic
COLD DRY
COOLING
COOL DRY
COLD [?]
COOLING
HOLOCENE OPTIMAL NORTHERN NEOLITHIC OPTIMUM

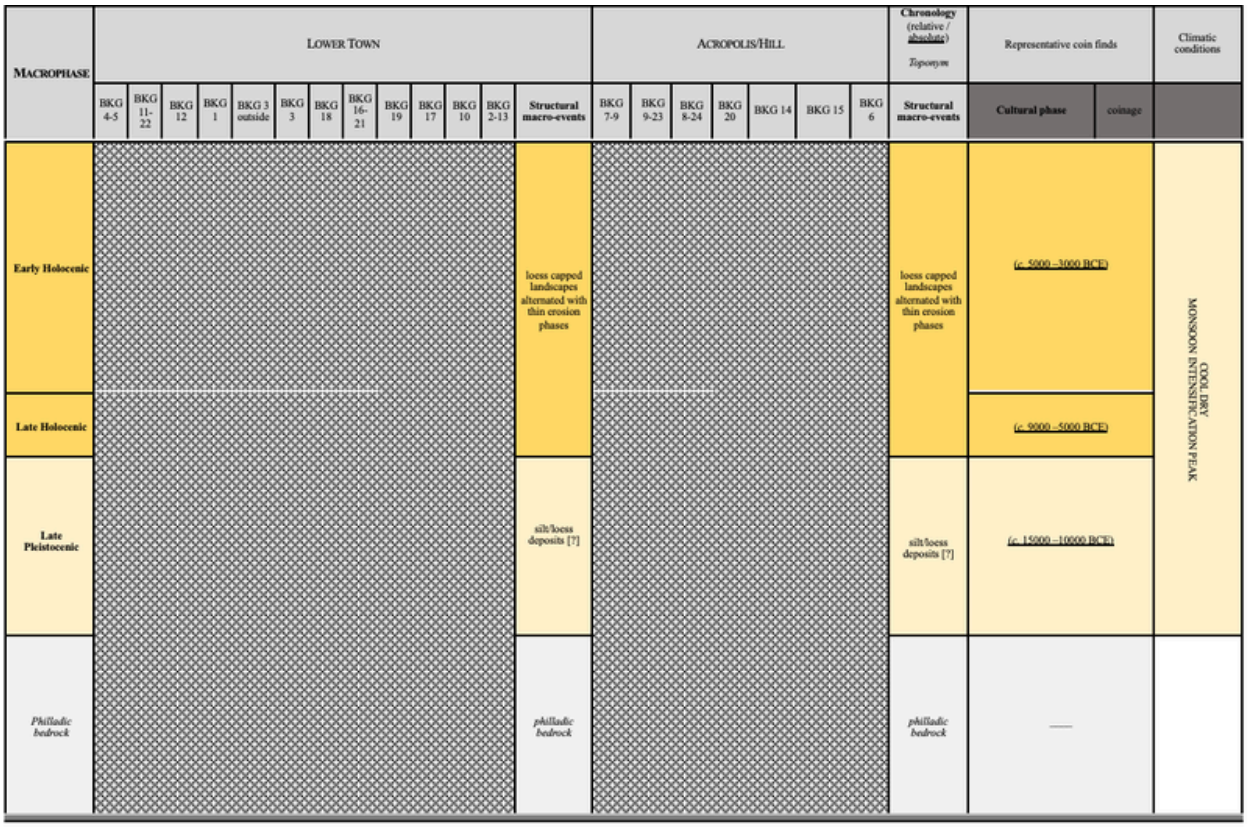

TABLE 1 – Concordance between the Macrophases of Barikot and the Periods/Phases of individual Trenches (L.M. Olivieri)

*The climatic data are all hypothetical and based on available information (see also Olivieri 2025b with refs)
**For radiocarbon data see TABLE 2.

Key:

Table 1. Periodization matrix of BKG excavated areas (Luca Maria Olivieri/IAMP, CC BY-NC-ND 4.0)

#	Macrophase	Sample ID	Source	Cal Date	relative probabilities (%)	1 σ	2 σ	Laboratory	Year	Material
80	Macrophase 9c-10	INNOVA-17	BKG 13 (26)	1517-1594 CE	80.0	x		INNOVA	2019	charcoal
79	Macrophase 9c	ENEA-185	BKG 2 (17)	1300-1330 CE	27.1			ENEA	2008	charcoal
				1340-1400 CE	41.1					
77	Macrophase 9b-9c	PSUAMS-6205	BKG 11 <1002>	1287-1393 CE	x			PSU	2019	bone
78		PSUAMS-4427	BKG 308 <139>	1276-1390 CE	x			PSU	2019	bone
75	Macrophase 9a	BETA - 664153	BKG 2_13_3	1113 – 1156 CE	32.3	x		BETA An	2023	soil
				1075-1108 CE	24.2	x				
				1028-1172 CE	95.4		x			
76		PSUAMS-6206	BKG 11 W (46)	1021-1154 CE	x			PSUAMS	2019	bone
85		FTMC-NS41-5	BKG 17 <F2> (17)	1083-1151 CE	56.6	x		VILNIUS RC	2024	bone
				1025-1160 CE	95.4		x			
97		BETA - 726618	BKG 6.3 (1846)	1026-1158 CE	95.4		x	BETA An	2025	seed
98		BETA - 726619	BKG 6.3 (1803)	1116-1219 CE	61.2		x	BETA An	2025	seed
				1042-1107 CE	34.2		x			
99	Macrophase 8b	BETA - 726622	BKG 24.1 (21)	951-1034 CE	84.5		x	BETA An	2025	charcoal
				896-923 CE	10.9		x			
69		ENEA-183	BKG 2 (344)	770–900 CE	55.6			ENEA	2008	charcoal
				920-960 CE	12.6					
70		ENEA-184	BKG 2 (365)	789-900 CE	47.7			ENEA	2008	charcoal
				910-960 CE	20.5					
71		DSH9629_CH	BKG 2 TT1E	873 CE	100.0	x		INNOVA	2019	charcoal
				894 CE	96.0		x			
106		DSH9646_CH	BKG 6.5 (38)	969-1018 CE	100.0	x		INNOVA	2019	charcoal
				942-1024 CE	84.0		x			
107		DSH9642_CH	BKG 6.5 (25)	886-991 CE	100.0	x		INNOVA	2019	charcoal
				944-975 CE	53.0		x			
108		DSH9574_WO	BKG 6.5 (25)	949-995 CE	70.0	x		INNOVA	2019	wood
				939–1018 CE	71.0		x			
109		DSH9575_SO	BKG 6.5 (55)	950-985 CE	62.0	x		INNOVA	2019	coprolyth (small mammal)
				891-994 CE	100.0		x			
110		DSH9635_CH	BKG 6.5 (23)	882-970 CE	100.0	x		INNOVA	2019	charcoal
				856-982 CE	86.6		x			
100		BETA - 726623	BKG 23.5 (48)	871-992 CE	81.5		x	BETA An	2025	charcoal
				828-860 CE	8.5		x			
				775-787 CE	5.4		x			
101		BETA - 726624	BKG 23.1 (218)	874-993 CE	88.2		x	BETA An	2025	charcoal
				830-852 CE	3.9		x			

#	Macrophase	Sample ID	Source	Cal Date	relative probabilities (%)	1 σ	2 σ	Laboratory	Year	Material
				775-786 CE	3.3		x			
67	Macrophase 8a	Sapienza (Callieri 2005: 423)	BKG 6.2 (477)	605-685 CE	x			ENEA	2005	charcoal
68		DSH9644_CH	BKG 6.5 (33)	690-750 CE	86.0	x		INNOVA	2019	charcoal
				670-778 CE	93.0		x			
74		DSH9647_CH	BKG 6.5 (41)	791-826 CE	34.0	x		INNOVA	2019	charcoal
				764-882 CE	78.0		x			
72		DSH9643_CH	BKG 6.5 (30)	774-884 CE	100.0	x		INNOVA	2019	charcoal
				800-872 CE	93.0		x			
73		DSH9645_CH	BKG 6.5 (35)	802-844 CE	52.0	x		INNOVA	2019	charcoal
				774-886 CE	100.0		x			
104		DSH9633_CH	BKG 6.5 (15)	802-844 CE	47.0	x		INNOVA	2019	charcoal
				770-895	97.0		x			
105		*DSH9634_CH*	*BKG 6.5 (17)*	*802–844 CE*	*51.0*	*x*		*INNOVA*	*2019*	*charcoal*
				775-888 CE	*100.0*		*x*			
65	Macrophase 7b	DSH9630_CH	BKG 13 (275)	693-746 CE	74.0	x		INNOVA	2019	charcoal
				688-752 CE	55.0		x			
66		DSH9631_CH	BKG 13 (294)	664-694 CE	71.0	x		INNOVA	2019	charcoal
				660-720 CE	72.0		x			
64	Macrophase 7a	DSH9632_CH	BKG 13 (299)	488-533 CE	67.0	x		INNOVA	2019	charcoal
				410-536 CE	100.0		x			
56	Macrophase 6	LTL12768A	BKG 11 W 7-8 68 (30)	250-350 CE	62.6	x		CEDAD	2012	bone
				220-420 CE	95.4		x			
57		LTL12772A	BKG 11 W 5-6 54 (393)	130-250 CE	68.2	x		CEDAD	2012	bone
				120-340 CE	94.2		x			
58		LTL12774A	BKG 11W 3-4 53 (226)	130-260 CE	59.5	x		CEDAD	2012	bone
				120-350 CE	95.4		x			
59		LTL12776A	BKG 11 W 7-8 63 (101)	125-230 CE	68.2	x		CEDAD	2012	bone
				70-260 CE	94.3		x			
60		LTL13055A	BKG 11 W 3-4 28 (600)	380-440 CE	46.0	x		CEDAD	2013	bone
				330-540 CE	95.4		x			
61		LTL13056A	BKG 11 W 3-428 (592	320-310 CE	45.7	x		CEDAD	2013	bone
				250-300 CE	22.5	x				
				240-410 CE	95.4		x			
62		LTL13057A	BKG 11 W 3-428 (597)	480-540 CE	36.5	x		CEDAD	2013	bone
				410-470 CE	31.7	x				
				380-550 CE	95.4		x			
63		LTL12775A	BKG 11 W 3-4 37bis (256)	130-240 CE	68.2	x		CEDAD	2013	bone
				280-330 CE	1.0	x				

#	Macrophase	Sample ID	Source	Cal Date	relative probabilities (%)	1 σ	2 σ	Laboratory	Year	Material
				70-260 CE	89.4		x			
	Macrophase 5b	x								
53	Macrophase 5a (H)	DSH11289_CH	BKG 168 (428)	156-237 CE	87.0	x		INNOVA	2022	seed
				116-252 CE	93.0		x			
54		DSH11248_CH	BKG 168 (428)	118-210 CE	96.0	x		INNOVA	2022	seed
				60-236 CE	99.0		x			
55		DSH11249_CH	BKG 168 (455)	110-250 CE	87.9	x		INNOVA	2022	seed
				8-362 CE	99.6		x			
52	Macrophase 4b-5a	DSH11245_CH	BKG 16 (165)	203-414 CE	96.0	x		INNOVA	2022	seed
				64-538 CE	100.0		x			
	Macrophase 4b	x								
51	Macrophase 4a	DSH11285_CH	BKG 160 (452)	3-84 CE	68.0	x		INNOVA	2022	seed
				54-204 CE	99.0		x			
46	Macrophase 3b	BKG 19.1-915	BKG 191 (915)			x		OXFORD	2023	seed
				BCE 56 - 20 CE	87.8		x			
47	Macrophase 3b (H)	DSH11290_CH	BKG 16 (332)	BCE 4 - 78 CE	76.0	x		INNOVA	2022	seed
	Macrophase 3b			BCE 54 - 130 CE	99.0		x			
48		DSH9648_CH	BKG 13 (350)	BCE 40-20 CE	100.0	x		INNOVA	2019	charcoal
				BCE 48-52 CE	100.0		x			
49		PSUAMS-6207	BKG 12 E (48)	BCE 47-52 CE	x			PSUAMS	2019	bone
50		DSH7906_SE	BKG 3 (592)	23-77 CE	100.0	x		INNOVA	2017	charcoal
				1-94 CE	90.0		x			
43	Macrophase 3a4	DSH7931_SE	BKG 11-K (1676)	BCE 204-164	86.8	x		INNOVA	2017	seed
				BCE 208-109	82.8		x			
44	Macrophase 3a4 (out cella H)	FTMC-RF53-8	BKG 16 E (731)	BCE 156-91	49.3	x		VILNIUS RC	2023	seed
				BCE 147-92	95.4		x			
45		FTMC-RF53-9	BKG 16 E (715)	BCE 178-97	56.1	x		VILNIUS RC	2023	seed
				BCE 202-51	88.3		x			
84		FTMC-NS41-1	BKG 16 SE (725)	BCE 174-96		x		VILNIUS RC	2024	seed
				BCE 201-48			x			
42	Macrophase 3a3-3a4	DSH7930_SE	BKG 11-K (2113)	BCE 208-109	76.4	x		INNOVA	2017	seed
				BCE 235-53	72.8		x			
102		DSH7612_SE	BKG 11-K (1687)	BCE 356-285	55.2	x		INNOVA	2017	seed
				BCE 235-171	43.9	x				
				BCE 369-106	100		x			
103		DSH7615_SE	BKG 11-K (1680)	BCE 297-228	61.1	x		INNOVA	2017	seed
				BCE 385-352	31.0					
				BCE 330-204	68.7					

#	Macrophase	Sample ID	Source	Cal Date	relative probabilities (%)	1 σ	2 σ	Laboratory	Year	Material
				BCE 395-334	31.3					
35	Macrophase 3a3	D-DSH7060	BKG 401 (328)	BCE 117-36	68.8	x		INNOVA	2016	bone
				BCE 193-28 CE	98.7		x			
36		D-DSH7061	BKG 401 (328)	BCE 174-91	92.1	x		INNOVA	2016	bone
				BCE 202-45	100.0		x			
37		D-DSH7060	BKG 401 (328)	BCE 163-128	40.0	x		INNOVA	2016	bone
				BCE 182-45	100.0		x			
38		ENEA-181	BKG 310 (592)	BCE 200-40 CE	68.2			ENEA	2005	charcoal
39		ENEA-182	BKG 302 (449)	BCE 180-70 CE	68.2			ENEA	2005	charcoal
40	Macrophase 3a3 (H)	FTMC-RF53-10	BKG 1615 = TT SW (924)	BCE 200-107	58.5	x		VILNIUS RC	2023	seed
				BCE 209-51	78.2		x			
41		FTMC-RF53-11	BKG 16 TTC (33)	BCE 176-97	57.7	x		VILNIUS RC	2023	seed
				BCE 201-51	88.9		x			
32	Macrophase 3a2	DSH7577_SE	BKG 11-K (1912bis)	BCE 210-156	51.5	x		INNOVA	2016	seed
				BCE 236-89	64.1		x			
33		OxA-38260	BKG 11-K (2131)			x		OXFORD	2019	seed
				BCE 359-214	95.4		x			
34		DSH7933_SE	BKG 11-K (2117)	BCE 204-161	75.9	x		INNOVA	2017	seed
				BCE 210-94	81.2		x			
	Macrophase 3a1	n								
29	Macrophase 2b (H)	BETA - 650199	BKG 16 (8) 2022	BCE 281-232	37.5	x		BETA An	2023	charcoal
				BCE 389-355	30.7	x				
				BCE 311-206	59.1		x			
				BCE 395-349	36.3		x			
30		DSH11243_CH	BKG 1615 (473)	BCE 290-209	66.0	x		INNOVA	2022	seed
				BCE 400-196	99.0		x			
83	Macrophase 2b (out cella H)	FTMC-NS41-2	BKG 16 SE (745)	BCE 357-278	39.7		x	VILNIUS RC	2024	seed
				BCE 233-101	53.2		x			
31	Macrophase 2b	DSH7926_SE	BKG 11-K (2153)	BCE 206-173	62.1	x		INNOVA	2016	seed
				BCE 214-156	53.2		x			
28		DSH7578_SE	BKG 12 W (206)	BCE 260-205	50.4	x		INNOVA	2016	seed
				BCE 369-201	100.0		x			
19	Macrophase 2a-2b (Shrine 16-H)	FTMC-RF53-1	BKG 16 TTC (40)	BCE 356-280	45.2	x		VILNIUS RC	2023	seed
				BCE 367-171	95.4		x			
20		FTMC-RF53-2	BKG 16 TTC (37)	BCE 355-281	45.8	x		VILNIUS RC	2023	seed
				BCE 365-170	95.4		x			
21		FTMC-RF53-4	BKG 16 TTC (21)	BCE 351-290	41.5	x		VILNIUS RC	2023	seed
				BCE 361-241	52.2		x			

#	Macrophase	Sample ID	Source	Cal Date	relative probabilities (%)	1 σ	2 σ	Laboratory	Year	Material
22		FTMC-RF53-6	BKG 16 TTC (1000)	BCE 397-359	48.7	x		VILNIUS RC	2023	seed
				BCE 403-351	54.2		x			
				BCE 293-208	41.2		x			
23		FTMC-RF53-10	BKG 16 TTC (41)	BCE 355-281	68.3	x		VILNIUS RC	2023	seed
				BCE 365-170	95.4		x			
81		FTMC-NS41-3	BKG 160 (2012)	BCE 375-290	15.2	x		VILNIUS RC	2024	bone
				BCE 290-209	53.1	x				
				BCE 389-342	24.2		x			
				BCE 321-201	71.2		x			
82		FTMC-NS41-4	BKG 160 [2000]	BCE 381-351	18.2	x		VILNIUS RC	2024	bone
				BCE 290-209	50.1	x				
				BCE 391-342	25.9		x			
				BCE 322-201	69.5		x			
24	Macrophase 2a-2b (16-H)	DSH11288_CH	BKG 1614 (414)	BCE 316-272	39.0	x		INNOVA	2022	seed
				BCE 384-195	99.0		x			
25		DSH11250_CH	BKG 1615 (278)	BCE 404-378	76.0	x		INNOVA	2022	seed
				BCE 413-358	61.0		x			
26		DSH11246_CH	BKG 1615 (483)-(485)	BCE 288-227	56.0	x		INNOVA	2022	seed
				BCE 322-200	66.0		x			
27		DSH11286_CH	BKG 1615 (483)	BCE 407-361	88.0	x		INNOVA	2022	seed
				BCE 422-384	67.0		x			
15	Marcophase 2a.2 (H)	DSH11247_CH	BKG 1615 (415)	BCE 540-362	99.0	x		INNOVA	2022	seed
				BCE 570-348	75.0		x			
16	Macrophase 2a.2	DSH7925_SE	BKG 11-K (2167)	BCE 399-385	100.0	x		INNOVA	2017	seed
				BCE 403-370	100.0		x			
18		DSH7954_C	BKG 11-K (2175)	BCE 494-410	89.5	x		INNOVA	2017	seed
				BCE 543-403	91.4		x			
12	Macrophase 2a1	DSH7928_SE	BKG 11-K (2182)	BCE 642-556	73.8	x		INNOVA	2017	seed
				BCE 654-541	61.9		x			
13		DSH7935_G	BKG 11-K (2184)	BCE 792-754	74.5	x		INNOVA	2017	bone
				BCE 608-595	13.8					
				BCE681-670	11.7					
				BCE 795-747	56.8		x			
				BCE 642-658	24.3					
				BCE 685-666	11.5					
				BCE 585-555	7.4					
				BCE 642-586	24.3					

#	Macrophase	Sample ID	Source	Cal Date	relative probabilities (%)	1 σ	2 σ	Laboratory	Year	Material
11	Interphase B	DSH7891_SE	BKG 11-K (2203)	BCE 651-544	66.0	x		INNOVA	2017	seed
				BCE 777-487	100.0		x			
14		DSH7893_SE	BKG 11-K (2196)	BCE 555-471	41.8	x		INNOVA	2017	seed
				BCE 747-385	33.9	x				
				BCE 597-411	55.8		x			
				BCE 755-680	27.0		x			
8	Macrophase 1b	DSH11244_CH	BKG 1614 (426)	BCE 930-832	100.0	x		INNOVA	2022	seed
				BCE 996-820	100.0		x			
9		PSUAMS-2786	BKG T1 (= Tucci)	BCE 921-831	n			PSUAMS	2019	bone
10		PSUAMS-2787	BKG T2 (= Tucci)	BCE 974-836	n			PSUAMS	2019	bone
4	Macrophase 1a-1b	OxA -38259	BKG 11-K (3016)-(3017)	BCE 1161-1056	95.4			OXFORD	2019	seed
5		OxA-38258	BKG 11-K (3014)	BCE 1125-926	95.4			OXFORD	2019	seed
6		DSH7579_SE	BKG 12 W (211)	BCE 1045-973	84.1	x		INNOVA	2016	seed
				BCE 1089-922	98.4		x			
7		DSH7929_SE	BKG 12 W (318)	BCE 1117-1044	100.0	x		INNOVA	2017	seed
				BCE 1129-1008	94.8		x			
1	Macrophase 1a	DSH7932_SE	BKG 12 W (306)	BCE 1291-1224	96.1	x		INNOVA	2017	seed
				BCE 1309-1209	82.2		x			
2		DSH7934_SE	BKG 12 W (305)	BCE 1122-1046	100.0	x		INNOVA	2017	seed
				BCE 1131-1011	90.0		x			
3		DSH7905_SE	BKG 12 W (310)	BCE 1114-1002	100.0	x		INNOVA	2017	seed
				BCE1131-929	94.2		x			
90	*= Interphase A (?)*	*BETA - 664158*	*BKG 2,13_16*	*BCE 1546 - 1511*	*33.0*	*x*		*BETA An.*	*2023*	*soil*
				BCE 1623 - 1501	*95.4*		*x*			
96	*= Macrophase 0*	*BETA - 664164*	*BKG 2,13_21*	*BCE 2569 - 2521*	*46.0*	*x*		*BETA An.*	*2023*	*soil*
				BCE 2499 - 2475	*22.2*	*x*				
				BCE 2581 - 2465	*94.0*		*x*			
88		*BETA - 664156*	*BKG 2,13_19*	*BCE 2102 - 2036*	*49.3*	*x*		*BETA An.*	*2023*	*soil*
				BCE 2150 - 2019	*82.1*		*x*			
93		*BETA - 664161*	*BKG 2,13_18*	*BCE 1972 - 1888*	*65.4*	*x*		*BETA An.*	*2023*	*soil*
				BCE 2027 - 1877	90.6		x			
92		BETA - 664160	BKG 2,13_10	BCE 2027 - 1941	68.2	x		BETA An.	2023	soil
				BCE 2040 - 1891	89.8		x			
86		BETA - 664154	BKG 2,13_12	BCE 2806 - 2754	38.3	x		BETA An.	2023	soil
				BCE 2815 - 2671	68.4		x			
				BCE 2895 - 2843	27.0		x			
87		BETA - 664155	BKG 2,13_13	BCE 2936 - 2897	40.9	x		BETA An.	2023	soil
				BCE 3021 - 2891	95.4		x			

#	Macrophase	Sample ID	Source	Cal Date	relative probabilities (%)	1 σ	2 σ	Laboratory	Year	Material
95	Holocenic deposits	*BETA - 664163*	*BKG 2,13_32*	*BCE 6368 - 6304*	*68.2*	*x*		*BETA An.*	*2023*	*soil*
				BCE 6585 - 6230	*95.4*		*x*			
91		BETA - 664159	BKG 2,13_14	BCE 6775 - 6651	66.4	x		BETA An.	2023	soil
				BCE 6831 - 6644	85.8		x			
94	Pleistocenic deposits	BETA - 664162	BKG 2,13_29	BCE 16215 - 16028	68.2	x		BETA An.	2023	soil
				BCE 16257 - 15928	95.4		x			
89		BETA - 664157	BKG 2,13_34	BCE 14952 - 14721	68.2	x		BETA An.	2023	soil
				BCE 15033 - 14630	95.4		x			

Legend – *Italics*: potentially contaminated/less reliable layers.
Samples from contaminated/unreliable layers are excluded from the list.
v. = *vacat*
% relative probability – confidence refers to value 1s

Table 2. List of radiocarbon measures (Luca Maria Olivieri/IAMP, CC BY-NC-ND 4.0)

At the excavated site of Barikot (see **Table 1**) chronostratigraphic complexes having substantial structural and material homogeneity for each given chronological period are grouped in Macrophases. Macrophases apply to all twenty-four trenches excavated up to 2024 (**Fig. 4**). Tables 1 and 2 illustrate the synopsis of the various internal phases/periods documented at Barikot and their absolute chronometric references (see also Olivieri et al. 2019).[4]

Chronology and Features of the Barikot Hill

The skyline of the summit or hilltop (942 meters a.s.l.) is heavily modified by artificial terraces and raised structures that partly filled the original sharply inclined profile.

Fig. 6. The eastern terrace of the Barikot hilltop seen from the east at the end of the excavation (IAMP, CC BY-NC-ND 4.0)

Fig. 7. The western terrace of the Barikot hilltop seen from the west during the excavations in 2024 (IAMP, CC BY-NC-ND 4.0)

The Barikot hill was occupied since prehistoric times. Evidence of Macrophase 0 pits (ca. 1700–1400 BCE) are reported from Trench BKG 9, while other materials attributed to this Macrophase were also unearthed in Trench BKG 8.[5] Structures and materials from Macrophase 1 (ca. 1200–800 BCE) were found both in Trenches BKG 14 (summit area) and 9 (on the West Terrace).[6] Evidence of an Indo-Greek defensive wall (Macrophase 3a) related to the acropolis fortification was documented on the West Terrace in Trenches BKG 7 and 9. Early structures and an ancient artificial terrace on which later structures were built were also documented on the Barikot summit (Macrophases 4–5; Trench BKG 14: Periods 1–3, cf. Minardi in chapter 14). The western and eastern sub-apical areas were also modified later than Macrophase 5. The East Terrace (**Fig. 6**) was heavily modified in Macrophase 8a. The West Terrace (**Fig. 7**) features a progressive terrace expansion from the Indo-Greek period (Macrophase 3a) to the Shahi and Ghaznavid phases (Macrophases 8a–b and 9a). Outside the West Terrace, on the northern side, a small cemetery datable to Macrophase 9b has been documented (see **Table 2**: no. 78).

Fig. 8. The hilltop and the East Terrace (top view from the north) (IAMP, CC BY-NC-ND 4.0)

Fig. 9. The East Terrace with Temple 6; view from above (north is to the right) (IAMP, CC BY-NC-ND 4.0)

The monumental East Terrace in Macrophase 8 presents an elevation of ca. 20 meters and an area development of 1,250 square meters (**Fig. 8**). A Buddhist sacred area stood here in Macrophases 5–7. On the ruins of this area, a religious building (Temple 6) was later built in Macrophase 8a (Callieri et al. 2000; Callieri et al. 2000–1) (**Fig. 9**). The podium of Temple 6 was elongated in Macrophase 8b.1 and again modified in Macrophase 8b.2 (cf. Casalini and Olivieri, chapter 16). One of these two episodes might be the one recorded in the inscription LM 119, which associates the renovation to the reign of Jayapala Deva (ca. 964–1001) (see **Fig. 5**).[7]

The sectors around the eastern and southeastern flanks of the hill are thick with ruins ranging from the Kushan period (remains of stupas and walls; Macrophases 4–5) to the Shahi, Ghaznavid, and Dardic periods (Macrophases 8–9) (**Fig. 10**).

a. Remains of wall **1** (17694/24).

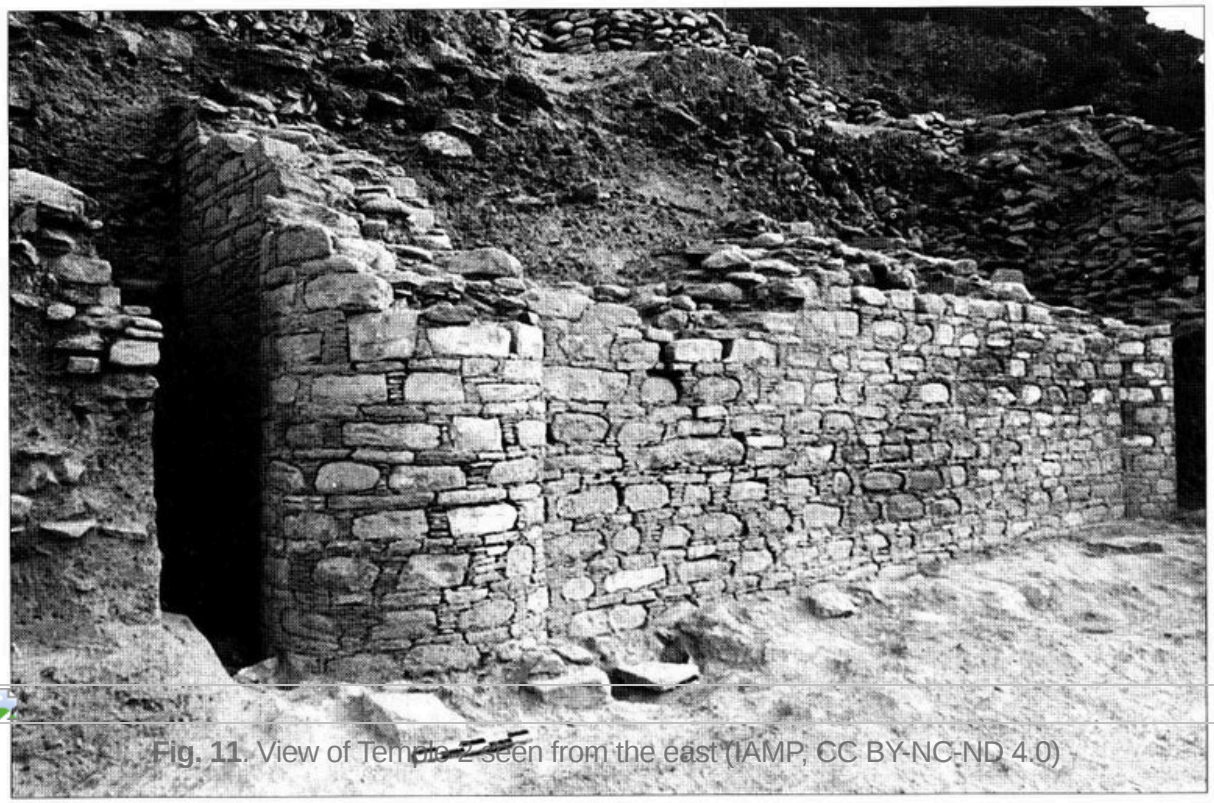

b. The tower building (room BKG 201) in trench BKG 2 at the beginning of the excavation (15534/30a; photo by A. Filigenzi).

Fig. 11. View of Temple 2 seen from the east (IAMP, CC BY-NC-ND 4.0)

The situation in the area at the southern foot of the hill is different, where there is evidence of a continuity of habitation that continues beyond the abandonment phase of the lower town (Macrophase 6), with Late Antique (Macrophase 7) and Shahi evidence. Here, in Macrophase 8b, there was a large palatial structure partially brought to light with a large wall marked by round bastions. From this protruded a square tower-like structure with a tetrastyle hypostyle hall and a ritual hearth, identified as a cult building (Temple 2) (**Fig. 11**). The area is occupied in Macrophase 9a with small buildings built on the slopes formed by the ruins of older structures. At the foot of the southern flanks of the hill there was an Islamic cemetery (11th–14th century; Narasinham et al. 2019; see **Table 2**: no. 78), which, after a phase of interruption (?) was used again from the sixteenth century until today. In Macrophase 9b, the entire area on the east, southeast, and south sides of the hill (Olivieri 2003a) was densely inhabited. In this period, a large agglomeration of tower-houses stood here, as the core of the pre-modern Dardic village of Beri-kot. A portion of that village has been excavated and dated. The abandonment of this village is dated to around the mid-sixteenth century (see **Table 2**: no. 80) (Olivieri 2023b).

The entire surface of the hill in its three sectors (East Terrace, West Terrace, summit) was the target of several excavation trenches (BKG 2, 6, 7, 8, 9, 13, 14, 15, 20E, 20N, 23, 24.1-5) (**Fig. 4**). The entire area was affected by periods of construction, remodeling, reconstruction, and transformation work, which is clearly visible throughout the area. These have been defined as Periods 0, 1, 2, 3, with sub-Periods (e.g., Period 2a). Period 0 corresponds to a long phase dated between the mid-second century BCE and mid-second century CE—that is, Macrophases 3a–b to 4. Period 1 corresponds to Macrophase 5, Period 2 to Macrophases 8a and 8b, Period 3 to Macrophase 9a. The later structures of Macrophase 9b are grouped under Period 4. The following pages refer mostly to Period 2a (late 7th–8th century or Turk Shahi) and 2b (early 9th–11th century or Hindu Shahi), that is, to Macrophases 8a and 8b.

Footnotes

1. Olivieri 2015: 52–53; Document no. 42. ↩
2. The earliest period of occupation of the hill is dated from the middle of the second millennium to the beginning of the first millennium BCE, i.e. in Macrophases 0 and 1 (see data and refs. in Olivieri et al. 2025). ↩
3. The entire upper structure of the hill is represented by garnet schists, studded everywhere with garnets emerging from the surface. This rock in the local Pashto is called "*periano gata*," the fairy stone. ↩
4. In terms of absolute dating Macrophase 0 refers to ca. 1700–1400 BCE, Macrophase 1 to ca. 1200–800 BCE, Macrophase 2 to ca. 500–200, Macrophase 3 to 150 BCE–70 CE, Macrophase 4 to 70–150 CE, Macrophase 5 to ca. 150–300 CE, Macrophase 6 to ca. 300–400 CE, Macrophase 7 to ca. 400–700 CE, Macrophase 8 to 700–1000 CE, Macrophase 9 to 1000–1500 CE, Macrophase 10 to 1500–1900 CE. ↩
5. See Olivieri and Micheli's contributions to Callieri et al. 2000. ↩

6. See, e.g., Olivieri, Minardi, and Vidale 2019 ↩

7. Other dedications for the construction of *devakules* associated with the name of Jayapala Deva include the well-known inscriptions from Udabhandra (Udabhandapura, Hund) (Sahni 1931–32; Rehman 1978) and other sites (Tucci 1970). ↩